



Universiteit
Leiden
The Netherlands

Positron emission tomography-derived metrics predict the probability of local relapse after oligometastasis-directed ablative radiation therapy

Greco, C.; Pares, O.; Pimentel, N.; Louro, V.; Morales, J.; Nunes, B.; ... ; Fuks, Z.

Citation

Greco, C., Pares, O., Pimentel, N., Louro, V., Morales, J., Nunes, B., ... Fuks, Z. (2022). Positron emission tomography-derived metrics predict the probability of local relapse after oligometastasis-directed ablative radiation therapy. *Advances In Radiation Oncology*, 7(2), 100864. doi:10.1016/j.adro.2021.100864

Version: Publisher's Version

License: [Creative Commons CC BY-NC-ND 4.0 license](https://creativecommons.org/licenses/by-nc-nd/4.0/)

Downloaded from: <https://hdl.handle.net/1887/3731086>

Note: To cite this publication please use the final published version (if applicable).

Scientific Article

Positron Emission Tomography–Derived Metrics Predict the Probability of Local Relapse After Oligometastasis-Directed Ablative Radiation Therapy



Carlo Greco, MD,^{a,*} Oriol Pares, MD,^a Nuno Pimentel, MD,^a Vasco Louro, MD,^a Javier Morales, MD,^a Beatriz Nunes, MD,^a Inês Antunes, MD,^a Ana Luisa Vasconcelos, MD,^a Justyna Kociolek, MD,^a Joana Castanheira, MD,^b Carla Oliveira, MD,^b Angelo Silva, MD,^b Sofia Vaz, MD,^b Francisco Oliveira, PhD,^b Eunice Carrasquinha, PhD,^c Durval Costa, MD,^b and Zvi Fuks, MD^{a,d}

^aDepartment of Radiation Oncology, Champalimaud Centre for the Unknown, Lisbon, Portugal; ^bDepartment of Nuclear Medicine-Radiopharmacology, Champalimaud Centre for the Unknown, Lisbon, Portugal; ^cComputational Clinical Imaging Group, Champalimaud Centre for the Unknown, Lisbon, Portugal; ^dMemorial Sloan Kettering Cancer Center, New York, New York

Received August 11, 2021; accepted November 5, 2021

Abstract

Purpose: Early positron emission tomography–derived metrics post–oligometastasis radioablation may predict impending local relapses (LRs), providing a basis for a timely ablation.

Methods and Materials: Positron emission tomography data of 623 lesions treated with either 24 Gy single-dose radiation therapy (SDRT) (n = 475) or 3 × 9 Gy stereotactic body radiation therapy (SBRT) (n = 148) were analyzed in a training data set (n = 246) to obtain optimal cutoffs for pretreatment maximum standardized uptake value (SUV_{max}) and its 3-month posttreatment decline (Δ SUV_{max}) in predicting LR risk, validated in a data set unseen to testing (n = 377).

Results: At a median of 21.7 months, 91 lesions developed LRs: 39 of 475 (8.2%) after SDRT and 52 of 148 (35.1%) after SBRT. The optimal cutoff values were 12 for SUV_{max} and –75% for Δ SUV_{max}. Bivariate SUV_{max}/ Δ SUV_{max} permutations rendered a 3-tiered LR risk stratification of dual-favorable (low risk), 1 adverse (intermediate risk) and dual-adverse (high risk). Actuarial 5-year local relapse-free survival rates were 93.9% versus 89.6% versus 57.1% (P < .0001) and 76.1% versus 48.3% versus 8.2% (P < .0001) for SDRT and SBRT, respectively. The SBRT area under the ROC curve was 0.71 (95% CI, 0.61–0.79) and the high-risk subgroup yielded a 76.5% true positive LR prediction rate.

Conclusions: The SBRT dual-adverse SUV_{max}/ Δ SUV_{max} category LR prediction power provides a basis for prospective studies testing whether a timely ablation of impending LRs affects oligometastasis outcomes.

Sources of support: This work had no specific funding.

Disclosures: Dr Greco reports nonfinancial support from Ceramedix Holdings and patent AN 62880797 outside the submitted work. Dr Fuks reports nonfinancial support from Ceramedix Holdings and patents US10413533B2, US20170333413A1, US20180015183A1, AN 62880797 outside the submitted work. All other authors have declared no conflicts of interest to disclose.

Research data are stored in an institutional repository and will be shared upon request to the corresponding author.

*Corresponding author: Carlo Greco, MD; E-mail: carlo.greco@fundacaochampalimaud.pt

<https://doi.org/10.1016/j.adro.2021.100864>

2452-1094/© 2021 The Authors. Published by Elsevier Inc. on behalf of American Society for Radiation Oncology. This is an open access article under the CC BY-NC-ND license (<http://creativecommons.org/licenses/by-nc-nd/4.0/>).

© 2021 The Authors. Published by Elsevier Inc. on behalf of American Society for Radiation Oncology. This is an open access article under the CC BY-NC-ND license (<http://creativecommons.org/licenses/by-nc-nd/4.0/>).

Introduction

The current practice of oligometastasis (OM)—directed ablation using stereotactic ablative radiation therapy is based on the notion that the oligometastatic syndrome represents a transitional phase in the spectrum of malignant progression from a purely localized primary tumor to wide metastatic dissemination.¹ The OM phenotype involves a limited cohort of slow-growing metastatic lesions in a state of metastatogenic equilibrium, and a corollary of this model postulates that OM ablation before polymetastatic escape occurs might lead to cancer cure.¹ Recent randomized clinical trials have shown that ablative OM consolidation improves OM progression-free survival and overall survival over standard of care.^{2–4} However, comparative efficacy and dose-impact studies of currently used ablative schedules are scarce. This issue has recently been addressed in a prospective phase III trial, randomizing OM-directed ablation with a standard 3×9 Gy hypofractionated stereotactic body radiation therapy (SBRT) regimen versus ultrahigh (24 Gy) single-dose radiation therapy (SDRT).⁵ Importantly, the tested treatment regimens fundamentally differ in the radiobiological mechanisms mediating tumor response. Whereas DNA double strand breaks (DSBs) constitute the lethal lesions after radiation exposure,⁶ the fractionated approach is based on progressive build-up of prolethal chromosomal instability associated with error-prone alternative end-joining of DSB lesions.⁷ In contrast, SDRT operates a dual-target tumor injury mechanism linking a transient microvascular vasoactive ischemia to tumor cell DNA damage, repressing homology-directed DSB repair. A synthetic DSB unrepaired and postmitotic tumor clonogen lethality leads to tumor lesion ablation.⁷

While ultrahigh (24 Gy) SDRT affords high rates of durable local control,^{8,9} its delivery is frequently restricted by an adjacent normal organ at risk (OAR) with dose/volume constraints that do not tolerate this dose intensity.¹⁰ In the presence of such dose conflicts, accepted rules prioritize prevention of OAR toxicity, mandating the use of SBRT schedules with reduced biological equivalent dose (BED) to meet the OAR specific tolerance.¹¹ However, such dose attenuation implies acceptance of a finite probability of in-field local lesion relapses (LRs).¹⁰ The phase III study randomizing 3×9 Gy SBRT versus 24 Gy SDRT revealed a statistically significant 4-fold increase of LRs in the SBRT arm with statistically significant increase in subsequent distant metastatic dissemination.⁵ While a comprehensive OM ablation mitigates progression of coexisting microscopic deposits into clinically overt metastatic lesions,⁵ the mechanism regulating this response

remains unknown. Hence, we posit that consolidative OM ablation should preferably be accomplished as early as feasible to maximize the repression of oligo- to polymetastatic conversion. The working hypothesis of the present study addresses this notion, arguing that an early identification of an impending in-field LR after an attempt of metastasis-directed ablation still represents an unmet clinical need. Here we explored whether positron emission tomography (PET)—derived molecular metrics obtained before and at 3 months postmetastasis-directed therapy may identify lesions at high risk for relapse, allowing a timely ablative consolidation of an otherwise potentially prometastatogenic active disease.

Methods and Materials

The present analysis of an institutional review board—approved, single-institution, clinical phase II non-randomized study of radioablation in oligometastatic disease (clinicaltrials.gov [NCT03543696](https://clinicaltrials.gov/ct2/show/study/NCT03543696)) deals with secondary endpoints not included in a previous report of this trial.¹² Briefly, between November 2011 and March 2017, 175 consecutive eligible patients with ≤ 5 OM lesions were treated and periodically followed as long as the patient maintained an oligometastatic status (ie, ≤ 5 concomitant lesions on follow-up PET/computed tomography [CT] scanning). At the time of the present analysis a total of 623 lesions were treated with ablative intent, an increase of 57 lesions from a previous report of this trial, resulting from an interim appearance and treatment of new OM lesions. Determination of the optimal cutoff for maximum standardized uptake value (SUV_{max}) decline was performed on the first 246 lesions treated during the first 36 months of the study until February 2015 constituting the training set,¹³ subsequently validated in a data set of 377 lesions previously unseen to testing.

Systemic therapy was permitted at the discretion of the treating physician. Patients with brain lesions were excluded from the study. The current analysis is restricted to pre- and posttreatment molecular PET/CT metrics affecting local tumor control. Patients were staged at protocol admission with ¹⁸F-FDG PET/CT scans, whereas prostate OM disease was staged with ⁶⁸Ga-PSMA. Detectable lesions were characterized in terms CT-derived gross tumor volume (GTV), location, and PET parameters.

PET/CT scan procedure

All patients had PET/CT scans performed according to standardized procedures, including a baseline scan for

staging workup and radiation therapy treatment-planning purposes and subsequent follow-up scans. Prior to each ^{18}F -FDG scan, patients were requested to fast for 6 hours before tracer administration. If blood glucose was lower than 200 mg/dL, ^{18}F -FDG (3.7-5 MBq/kg of patient weight) was injected using an automatic injector (Intego, Medrad Inc). All patients injected with ^{18}F -FDG were followed in strict resting conditions for a minimum of 60 minutes. Patients who received ^{68}Ga -PSMA needed no specific preparation, and scans were acquired at 60 minutes postinjection.

The PET/CT scan (Gemini TF, Philips) was acquired with a low-dose CT (120-140 kV, 60 mA per rotation) from the skull base to the upper third of the thighs. PET data were obtained thereafter on 3-dimensional mode. Quantitative SUV evaluation was performed within the volumetric region of interest (Extended Brilliance Workspace algorithm NM 2.0 AB-V5.4.3.40140, Philips). The standardized uptake value for the voxel with the highest activity concentration (SUV_{max}) was recorded. Tumor response was scored based on modified PERCIST criteria, with metabolic relapse defined as any increase of $\text{SUV}_{\text{max}} > 30\%$ above nadir level. All metabolic relapses were confirmed by morphologic CT imaging. All lesions had a minimum of 2 posttreatment scans.

Radioablation

Treatment planning and delivery techniques used were strictly standardized and have been described before.¹² Briefly, patients were placed on dedicated repositioning devices and scanned using 2 mm slice thickness CT images on the PET/CT scanner. A 4-dimensional CT acquisition was performed to allow visualization and assessment of internal organ motion to be accounted for during treatment planning according to the RTOG 0236 guidelines. The GTV was delineated and expanded with an isotropic 3 mm margin to generate the treatment planning volume. Treatment planning (Eclipse, Varian Medical Systems, Palo Alto, CA) used 2 to 4 coplanar high dose-rate flattening filter-free photon beams (6 or 10 MV) in all cases. Heterogeneity corrections were used to ensure appropriate dose calculation. While 24 Gy SDRT was the preferred regimen in the study, 3×9 Gy SBRT was used when OAR dose/volume constraints did not allow safe implementation of SDRT. The same treatment planning guidelines were used for both regimens. All plans underwent strict quality assurance testing with a pretreatment phantom dry run (ArcCHECK, Sun Nuclear Corp, Melbourne, FL). Gamma index analysis values at the 3%/3 mm $\geq 90\%$ were considered acceptable. The Edge/True-Beam STx platforms (Varian Medical Systems, Palo Alto, CA) were used for treatment delivery. A 6° of freedom couch enabled accurate correction of rotational discrepancies. Setup accuracy was performed by on-board cone beam CT matching with the reference planning CT before treatment

delivery. Any discrepancies in target position ≥ 1 mm or ≥ 1 degree relative to the planning CT scan were corrected and verified with additional cone beam CT scans.

Endpoints

Radiotracer uptake values were recorded for each lesion at baseline and every follow-up scan. The change in maximum standardized uptake value ($\Delta\text{SUV}_{\text{max}}$) was calculated with respect to the baseline value at the 3- and 6-month posttreatment time points. Local response to treatment was scored as complete response, partial response, stable disease, or failure based on modified PERCIST criteria (ie, any increase of $\text{SUV}_{\text{max}} > 30\%$ above nadir level within the irradiated volume).¹⁴ If posttreatment PET showed no residual abnormal uptake with SUV_{max} decline $> 90\%$ the lesion was scored a complete metabolic response.

Statistical analysis

Time to local failure was calculated from the day of treatment. Pretreatment SUV_{max} and $\Delta\text{SUV}_{\text{max}}$ were used in the confirmatory analysis. In a complementary analysis GTV, OM lesion histology, target site, and use of systemic therapy before treatment or postablation were also tested as variables affecting local control. All statistical tests were 2-tailed with a significance level (α) = 0.05. Estimates of local relapse-free survival (LRFS) were calculated using the Kaplan-Meier method. Univariate analysis with continuous and discrete variables were used to explore associations with LRFS, and a stepwise multivariable model was set to estimate the association of covariates with impending LR, using the Cox proportional hazard method. Hazard ratio (HR) and 95% confidence intervals (95% CI) were obtained. Receiver operating characteristic (ROC) analysis was performed on variables with significant association with impending LR. The choice of cutoff points to convert continuous covariates into a binary partitioning used the method of Contal and O'Quigley,¹⁵ which provides an objective dichotomization via maximizing the HRs of partitioning values based on log-rank statistics to estimate optimal outcome-oriented cutoff points. Statistical computations were performed using R software version 3.4.4 (R Project for Statistical Computing) or GraphPad Prism 8.0 software (Prism Inc, Reston, VA).

Results

Lesion characteristics

Table 1 provides basic details on lesion characteristics. A total of 623 lesions were treated, 475 (76%) with 24 Gy SDRT and 148 (24%) with 3×9 Gy SBRT. There were

Table 1 Lesion characteristics

	No. (%)	No. (%)	No. (%)
	All	Single-dose radiation therapy	Stereotactic body radiation therapy
	623 (100)	475 (76)	148 (24)
Histology			
Prostate	147 (24)	124 (26)	23 (16)
Non-small cell lung cancer	115 (18)	83 (18)	32 (22)
Colorectal cancer	92 (15)	71 (15)	21 (13)
Breast	83 (13)	64 (13)	19 (13)
Renal cell	30 (5)	25 (6)	5 (3)
Endometrial	20 (3)	4 (1)	16 (11)
Urothelial	17 (3)	11 (2)	6 (4)
Small cell lung	17 (3)	13 (3)	4 (3)
Sarcomas	16 (3)	13 (3)	3 (2)
Ovarian	14 (2)	14 (3)	0 (0)
Pancreas	14 (2)	10 (2)	4 (3)
Other (<10/histology)	42 (6)	30 (6)	12 (8)
Lesion site			
Bone	203 (32)	165 (35)	38 (26)
Lymph nodes	215 (35)	130 (27)	85 (57)
Lung	112 (17)	102 (21)	10 (7)
Liver	41 (8)	36 (8)	6 (4)
Soft tissues	51 (8)	42 (9)	9 (6)
Concomitant systemic treatment	181 (29)	140 (29)	41 (28)
Lesion volume			
Median	5.1	4.8	7.5
Mean \pm 1 SD	15.6 \pm 37.8	7.9 \pm 6.9	27.6 \pm 63.8
Maximum standardized uptake value			
Median	6.8	6.7	7.5
Mean \pm 1 SD	9.2 \pm 8.4	8.9 \pm 8.3	10.2 \pm 8.7
Change in maximum standardized uptake value			
Median	−79.2%	−80.0%	−75.9%
Mean \pm 1 SD	−66.7% \pm 32.5%	−66.2 \pm 33.7%	−67.8% \pm 28.3%

Abbreviation: SD = standard deviation.

no statistically significant differences in median baseline SUV_{max} and ΔSUV_{max} among different histologies, except for renal cell carcinoma, which displayed reduced median values ($P < .001$). All lesions had PET/CT planning scans and a minimum of 2 posttreatment scans (median 5; mean 5; range 2-12). Concomitant systemic therapy did not significantly affect postablative ΔSUV_{max} in either radiation regimen ($P = .74$).

At a median follow-up of 21.7 months (range, 6-86.5) 91 of 623 lesions (14.6%) developed evidence of LR within

the treated field. Median follow-up for lesions that did not develop LR was 22.7 months (range, 6-86.5). Lesions ablated with SDRT had an actuarial 8.2% (39 of 475) incidence of LR versus 35.1% (52 of 148) for SBRT-treated lesions ($P < .0001$). Median time to local relapse for the SDRT cohort was 10.2 months (mean, 10.6; range, 3-27.1) and 12.1 months (mean, 14.0; range, 4.9-46.6) for SBRT.

Of 54 patients with in-field LRs, 19 (35%) with a total of 23 lesions were eligible for salvage reirradiation, whereas 4 (7%) were managed surgically. Patients with

LRs concomitant with polymetastasis progression (≥ 6 lesions: 22 patients, 41%) or patients with restrictive comorbidities (9 patients, 17%) were not considered candidates for LR salvage. A total of 16 lesions were reablated with SDRT (12 relapsing after SBRT and 4 after SDRT) and 7 with SBRT (5 relapsing after SBRT and 2 after SDRT). Of the 23 salvaged lesions, 8 (35%) relapsed at a median of 7.6 months, that is, 4 of 16 (25%) after SDRT versus 4 of 7 (57%) after SBRT. There were no grade 3 to 4 adverse events in patients who received reablation with either 3×9 Gy SBRT or 24 Gy SDRT as the salvage regimen.

Training set

The training set consisted of 246 radioablated lesions. To establish and quantify the baseline SUV_{max} and the postablative ΔSUV_{max} optimal values in predicting LRFS, these continuous variables were partitioned into binary subgroups to derive the most significant cutoff values associated with a clinically confirmed in-field LR.¹⁵ The analysis yielded an optimal SUV_{max12} cutoff value of 12 (SUV_{max12}), separating the actuarial LRFS into 79.3% versus 58.0% (HR, 0.25; 95% CI, 0.12-0.55; $P = .0003$), with the higher SUV_{max} having a worse prognosis. The 3-month postablative ΔSUV_{max} decline of 75% cutoff ($\Delta SUV_{75\%}$) separated actuarial LRFS into 84.2% versus 67.2% (HR, 0.34; 95% CI, 0.19-0.62; $P = .0002$), with the larger declines having a better prognosis. Furthermore, to test whether the treatment regimen effected the cutoff values, we found that for the 201 SDRT-treated lesions the SUV_{max12} separated the cohort into 91.6% versus 74.9% (HR, 0.36; 95% CI, 0.04-0.64; $P = .007$) and $\Delta SUV_{75\%}$ into 94.1% versus 83.6% (HR, 0.38; 95% CI, 0.14-0.98; $P = .03$). For the 45 lesions treated with 3×9 Gy SBRT,

the SUV_{max12} did not provide a significant separation, although the $\Delta SUV_{75\%}$ yielded 76.3% versus 28.7% (HR, 0.38; 95% CI, 0.15-0.93; $P = .003$).

Validation of statistically previously unseen data

The median GTV in the validation set was smaller than in the training set (4.0 vs 6.1 cm^3 ; $P = .003$). However, there was no statistically significant difference in baseline SUV_{max} (6.9 vs 6.7, respectively; $P = .91$). In the 377 lesions previously unseen to testing, the pretreatment SUV_{max12} revealed a separation of actuarial LRFS of 85.0% versus 68.1% (HR, 0.56; 95% CI, 0.27-1.18; $P = .90$), whereas the $\Delta SUV_{max75\%}$ cutoff yielded a separation of 89.1% versus 73.1% in actuarial LRFS rates (HR, 0.24; 95% CI, 0.13-0.44; $P < .0001$). Further analysis of $\Delta SUV_{max75\%}$ in 274 SDRT-treated lesions showed that actuarial LRFS was 94.7% versus 82.6% (HR, 0.28; 95% CI, 0.11-0.57; $P = .002$; Fig 1A). Similarly, Figure 1B shows LRFS separation by $\Delta SUV_{max75\%}$ in 103 SBRT-treated lesions of 82.8% versus 31.2% (HR, 0.11; 95% CI, 0.05-0.24; $P < .0001$).

Validation of ^{18}F -FDG versus ^{68}Ga -PSMA cutoffs

A set of complementary analyses was designed to ensure that the baseline SUV_{max} and ΔSUV_{max} cutoff values defined previously were compatible for both PET tracers. The median baseline SUV_{max} was 7 versus 6.2 for ^{18}F -FDG versus ^{68}Ga -PSMA ($P = .10$). The optimal pretreatment SUV_{max} cutoff value for ^{18}F -FDG was 13 (LRFS, 79.1% vs 65.1%; HR, 0.39; 95% CI, 0.22-0.70; $P = .0008$),

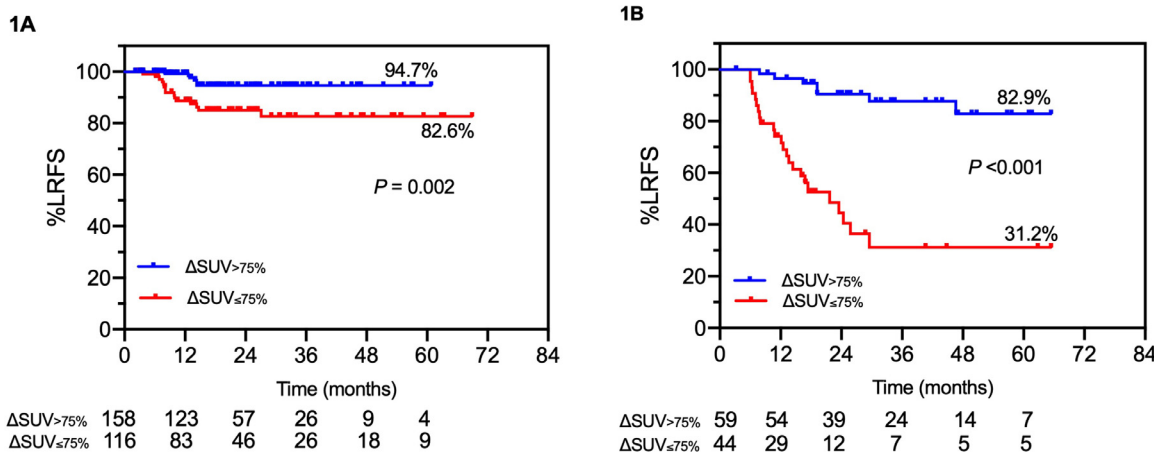


Fig. 1 Validation of ΔSUV_{max} for 2 radioablative regimens. (A) Actuarial LRFS of lesions ablated with metastasis-directed 24 Gy single-dose radiation therapy. (B) Three sessions of 9 Gy stereotactic body radiation therapy dichotomized by the optimal positron emission tomography 3-month posttreatment ΔSUV_{max} cutoff value of 75% decline. *Abbreviations:* LRFS = local relapse-free survival; ΔSUV_{max} = change in maximum standardized uptake value.

whereas the best cutoff value for ^{68}Ga -PSMA was 11 (LRFS, 92.6% vs 72.4%; HR, 6.5; 95% CI, 1.38-30.35; $P = .01$). Nonetheless, Figure 2A and Figure 2B show that pretreatment $\text{SUV}_{\text{max}12}$ still reveals statistically significant separations for both PET tracers.

The median 3-month $\Delta\text{SUV}_{\text{max}}$ was -75.2% versus -84.3% for ^{18}F -FDG versus ^{68}Ga -PSMA ($P = .01$). Figure 2C shows $\Delta\text{SUV}_{\text{max}75\%}$ was a significant predictor of LRFS for ^{18}F -FDG (LRFS, 85.1% vs 69.5%; HR, 0.33; 95% CI, 0.17-0.62; $P = .0001$). Despite the paucity of LR events in the ^{68}Ga -PSMA-assessed prostate lesions (11 of 147, 7.5%), the $\Delta\text{SUV}_{\text{max}75\%}$ cutoff still revealed a significant separation (Fig 2D; LRFS, 98.7% vs 72.8%; HR, 0.08; 95% CI, 0.02-0.29; $P < .0001$).

Univariate, multivariate, and ROC analyses

While we showed the binary-partitioned $\text{SUV}_{\text{max}12}$ and $\Delta\text{SUV}_{\text{max}75\%}$ were positively associated with LRFS,

univariate and multivariate analyses were performed to test whether additional variables were associated with increased LR risk (Table 2). In addition, ROC analyses were performed to determine the sensitivity and specificity of these variables. GTV size was positively associated with LR as a continuous variable in both regimens (Cox regression; SDRT, $P = .009$; SBRT, $P = .006$). However, the effect of GTV derived by the area under the ROC curve was only slightly superior to 0.5 (AUC = 0.60, 95% CI, 0.53-0.66 for entire cohort; AUC = 0.65, 95% CI, 0.56-0.73 for SDRT; AUC = 0.51, 95% CI, 0.41-0.61 for SBRT). Posttreatment $\Delta\text{SUV}_{\leq 75\%}$ was also confirmed as an independent predictor of LR in the multivariate analysis for both regimens (Cox regression for SDRT, $P = .008$, and for SBRT, $P < .0001$). The areas under the ROC curve were acceptably discriminating at 0.65 (95% CI, 0.57-0.74) and 0.69 (95% CI, 0.60-0.78) for the SDRT- and SBRT-treated lesions, respectively. For the optimal cut-off of 75% decline, the sensitivity and specificity were, respectively, 71.8% and 57.7% for the SDRT-treated lesions and 75.0% and 67.7% for the SBRT-treated lesions.

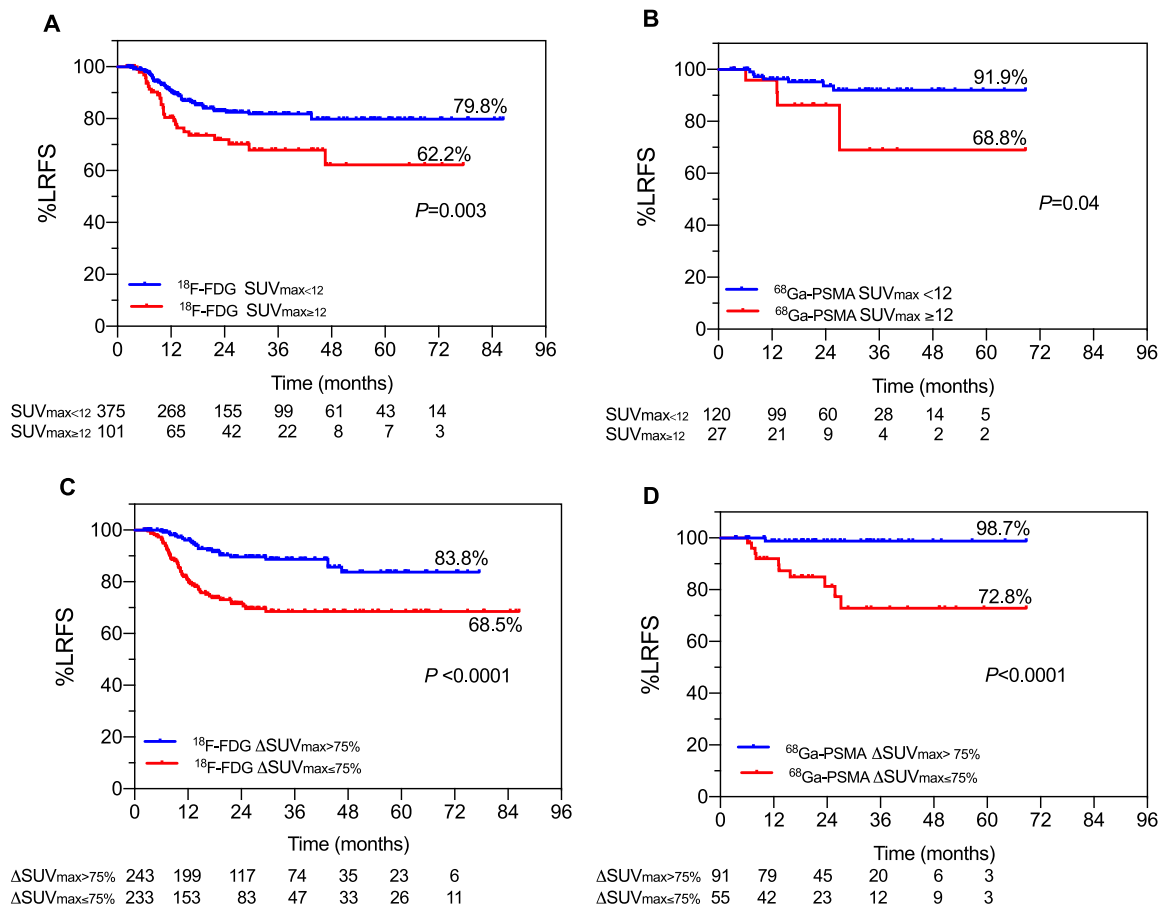


Fig. 2 Validation of cutoff values for ^{18}F -FDG and ^{68}Ga -PSMA. (A, B) Actuarial LRFS of radioablated lesions as a function of pretreatment SUV_{max} using a cutoff value of 12 for ^{18}F -FDG (A) and ^{68}Ga -PSMA (B). (C, D) Actuarial LRFS of radioablated lesions as a function of 3-month posttreatment $\Delta\text{SUV}_{\text{max}}$ cutoff value of $>75\%$ declines for ^{18}F -FDG (C) and ^{68}Ga -PSMA (D). *Abbreviations:* LRFS = local relapse-free survival; SUV_{max} = maximum standardized uptake value; $\Delta\text{SUV}_{\text{max}}$ = change in maximum standardized uptake value.

Table 2 Univariate and multivariate analyses

24 Gy single-dose radiation therapy								
Variable	Univariate 95% CI				Multivariate 95% CI			
	Hazard ratio	Lower	Upper	P value	Hazard ratio	Lower	Upper	P value
Histology								
Other histology (reference)								
Breast	0.300	0.065	1.373	0.121	0.287	0.059	1.402	0.123
Colorectal cancer	2.636	1.138	6.105	0.023	2.669	1.053	6.763	0.038
Non-small cell lung cancer	1.734	0.735	4.090	0.208	1.677	0.668	4.209	0.270
Prostate	0.380	0.119	1.212	0.102	0.419	0.121	1.447	0.169
Lesion site								
Bone (reference)								
Liver	2.077	0.561	7.676	0.273	0.520	0.093	2.909	0.457
Lymph node	1.201	0.476	3.027	0.697	1.360	0.476	3.886	0.565
Lung	2.208	0.914	5.330	0.078	1.340	0.515	3.481	0.547
Soft tissues	3.489	1.297	9.383	0.013	2.090	0.714	6.117	0.178
Volume								
Gross tumor volume (cm ³) continuous	1.009	1.002	1.016	0.009	1.008	0.998	1.018	0.111
Baseline SUV_{max}								
SUV _{max} continuous	1.012	0.981	1.043	0.457	1.006	0.883	1.145	0.926
SUV _{max} cutoff	1.311	0.698	2.461	0.399	1.086	0.481	2.452	0.841
Posttreatment SUV_{max}								
Delta ≤75%	0.292	0.145	0.586	<0.001	0.280	0.109	0.719	0.008
Difference pre/posttreatment	0.992	0.949	1.039	0.754	1.016	0.884	1.168	0.819
3 × 9 Gy stereotactic body radiation therapy								
Histology								
Other histology (reference)								
Breast	0.558	0.210	1.483	0.242	0.543	0.210	1.462	0.226
Colorectal cancer	1.844	0.859	3.958	0.116	1.800	0.828	3.901	0.137
Non-small cell lung cancer	0.970	0.417	2.255	0.943	0.970	0.408	2.218	0.908
Prostate	1.131	0.442	2.893	0.796	1.110	0.438	2.791	0.829
Lesion site								
Bone (reference)								
Liver	0.000	0.000	Infinite	0.996	0.000	0.000	Infinite	0.997
Lymph node	0.921	0.470	1.803	0.810	1.240	0.590	2.582	0.574
Lung	2.003	0.749	5.359	0.166	1.110	0.397	3.107	0.841
Soft tissues	1.274	0.358	4.522	0.708	1.300	0.353	4.769	0.694
Volume								
Gross tumor volume (cm ³) continuous	1.006	1.001	1.010	0.006	1.010	1.002	1.010	0.003
Baseline SUV_{max}								
SUV _{max} continuous	1.098	0.983	1.227	0.096	1.110	1.982	1.227	0.097
SUV _{max} cutoff	0.906	0.436	1.881	0.791	0.908	0.436	1.881	0.792
Posttreatment SUV_{max}								
Delta ≤75%	0.150	0.057	0.388	<0.001	0.165	0.063	0.427	<0.001
Difference pre/posttreatment	0.929	0.814	1.060	0.275	0.929	0.801	1.060	0.275

Abbreviations: CI = confidence interval; SUVmax = maximum standardized uptake value.

Bivariate combinations of baseline and posttreatment SUV_{max} declines

For these studies the training and the validation sets were combined using the validated optimized cutoff values. Due to the preponderant effect of ΔSUV_{max} and the relative paucity of events in the SDRT cohort, addition of either GTV or pretreatment SUV_{max} did not improve the predictive value of ΔSUV_{max} alone, and a subset of lesions at very high risk of LR could not be identified with pre- and 3-month post-SDRT PET/CT metrics (93.9% vs 89.6% vs 57.1%; $P < .0001$). However, for the more relapse-prone SBRT-treated lesions, the use of bivariate permutations of baseline SUV_{max12} and $\Delta SUV_{max75\%}$ resulted in area under the ROC curve of 0.71 (95% CI, 0.61-0.79; Fig 3A). The combination of no adverse features (ie, pretreatment $SUV_{max} < 12$ and ΔSUV_{max} declines $> 75\%$, designated here as low risk) versus the presence of 1 adverse covariate (intermediate risk) or dual-adverse $SUV_{max} > 12$ and ΔSUV_{max} declines $\leq 75\%$ (high-risk) resulted in a 3-tiered actuarial 5-year LRFS stratification (Fig 3B; log-rank $P < .0001$), yielding a 76.5% true positive LR prediction rate. Of note, the distributions of LRs by risk category did not significantly change at the 6-month assessment (Fig 3C) and the dual-adverse subgroup included the same lesions identified at 3 months, suggesting that early identification of the lesions at high risk for relapse is feasible.

Discussion

The present study confirms $\Delta SUV_{max75\%}$ is a strong predictor of freedom from local failure, independently verified in a large subset of lesions previously unseen to testing. Univariate and multivariable analysis of the entire cohort indicates that $\leq 75\%$ ΔSUV_{max} declines is the sole independent PET metric predictor of local failure post-radioablation. Additionally, $\Delta SUV_{max75\%}$ in combination with baseline SUV_{max} defines a 3-tiered LR risk at 3 months postablation, where the dual-adverse $SUV_{>12}/\Delta SUV_{\leq 75\%}$ category yields a robust association with impending true LRs in the 3×9 Gy SBRT cohort. The fact that the 3-tiered stratification at 3 and 6 months yielded similar results in the high-risk category supports the notion that early identification of impending LRs is feasible. Published data on the use of pre- and posttreatment PET metrics to evaluate response to ablative radiation therapy are scant.¹⁶⁻¹⁹ The present development of a PET-based algorithm that predicts in-field recurrences with high specificity and sensitivity provides an approach to prospectively test the hypothesis that a timely consolidative radioablation of relapsing OM lesions effects the natural history of preexisting microscopic OM foci, mitigating their metastatogenic conversion.

There is a need for such an approach, as lesions untreatable with high-BED regimens are at a higher risk for in-field LRs, hypothetically associated with an increase in subsequent distant metastatic dissemination.⁵ While at present there are no experimental animal models of the human OM syndrome, and advancement in the field depends on clinical experimentation, there is nonetheless substantial evidence indicating that the oligometastatic state is a biologically dynamic process, which engages regulators of the OM metastatogenic equilibrium, gradually increasing a propensity toward a polymetastatic switch.^{20,21} Consistent with this notion, the outcomes of the randomized SBRT versus SDRT OM study⁵ suggest that functional activity of unattended or relapsing OM residua, presumably expressing increased prometastatogenic propensity, appear to promote polymetastatic conversion of the preexisting microscopic OM deposits.^{20,21} Hence, we posited that early detection of an unsuccessful initial ablation, proven feasible in the present studies, might render benefit from ablative consolidation as early as possible, if deemed clinically safe.

At present, the tolerance of reirradiation with ablative doses at 3 months after radiation therapy is unknown. While previous experience indicates that reirradiation of clinically detected in-field LRs is feasible and safe with $< 5\%$ grade 3 adverse events,²²⁻²⁵ the tolerance of consolidative reablation at 3 months will have to be tested in a phase I feasibility and toxicity study. Preliminary data indicate that OM lesions in so-called parallel organs,^{26,27} such as the lung and liver, can be safely reirradiated with ablative intent,²² although centrally located chest relapses require strict adherence to safe OAR dose/volume constraints.²⁸ With regard to the so-called serial OARs,^{26,27} data emerging for spinal lesions suggest that SBRT salvage can be safely delivered at ≥ 5 months after initial treatment, provided strict dose/volume constraints for the spinal cord are met.²⁹ A multi-institutional pooled analysis of spine reirradiations after conventional fractionation (median dose/fractions, 30 Gy/10) used 18 Gy single dose in 60% of the cohort,³⁰ reporting no radiation-induced myelopathy or radiculopathy. Our recently published data reported that 1-year local control was significantly improved (90% vs 73%) in lesions re-treated with 24 Gy SDRT compared with 3×9 Gy SBRT.¹² A study of salvage SBRT (median 30 Gy/4 fractions) at a median of 6.8 months for in-field failure after initial SBRT (median 24 Gy/2 fractions) reported 81% 1-year local control with no cases of radiation-induced myelopathy or vertebral compression fracture.³¹ While preliminary reports on salvage reablation in overt relapses are encouraging, we contend that the 3-month PET/CT readily detects the residual postablation tumor, with a frequently smaller GTV than at baseline, facilitating avoidance of adjacent OARs, and thus permitting early ablative consolidation with ultrahigh dose SDRT, if indicated. However, even if proven to be well tolerated, unnecessary reirradiation of false positive lesions should obviously be maximally avoided.

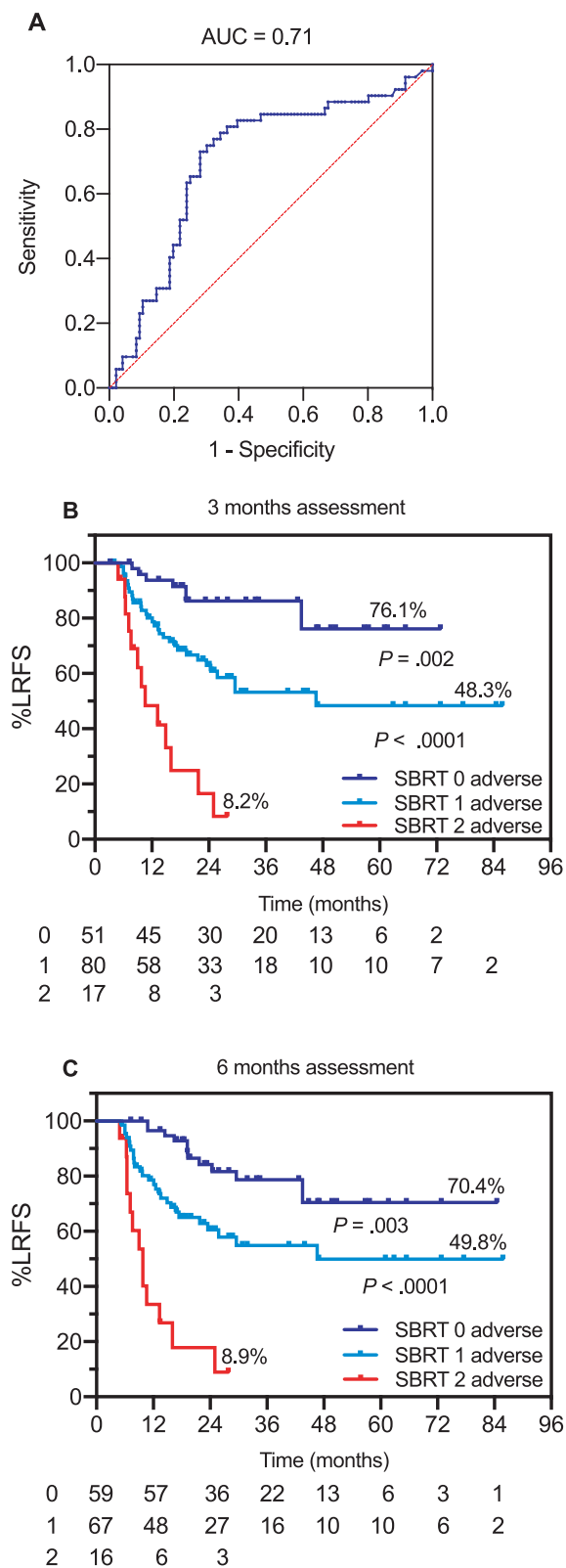


Fig. 3 SBRT-treated lesions. (A) Area under the receiver operating characteristic curve for pretreatment SUV_{max} and 3-month ΔSUV_{max} . (B, C) Actuarial LRFS of predictive model with posttreatment assessment at 3 (B) and 6 months (C) using permutations of adverse features to stratify lesions into prognostic groups: 0 adverse designates lesions with baseline $SUV_{max} < 12$ and posttreatment $\Delta SUV_{max} > 75\%$ declines; 1 adverse designates lesions with either $SUV_{max} \geq 12$ or $\Delta SUV_{max} \leq 75\%$ decline; and 2 adverse designates lesions with both ≥ 12 and $SUV_{max} \leq 75\%$ decline. *Abbreviations:* AUC = area under the curve; LRFS = local relapse-free survival; SBRT = stereotactic body radiation therapy; SUV_{max} = maximum standardized uptake value; ΔSUV_{max} = change in maximum standardized uptake value.

Conclusion

In the present study, molecular metrics in the context of 24 Gy SDRT were poorly discriminating, likely because of a significantly lower frequency of LR events with this regimen, and the possible presence of confounding post-treatment inflammatory phenomena after ultrahigh dose exposure, presumably impacting the specificity of LR prediction by $\Delta\text{SUV}_{\text{max}}$ intensity.^{32,33} OM lesions actively engaged in postmitotic tumor cell lethality are known to elicit an intense stromal inflammatory response and to avidly accumulate ^{18}F -FDG.³⁴ In contrast, the low BED regimen of 3×9 Gy SBRT adopted here as indispensable in meeting dose/volume restrictions of incidental OARs is less likely to activate nonspecific tracer uptake and influence $\Delta\text{SUV}_{\text{max}}$ intensity. However, the linear quadratic α/β_{10} -based calculation (BED₁₀) 3×9 Gy corresponds to 51.3 Gy, documented as low in the BED spectrum of hypofractionated SBRT regimens, hence the high LR rates associated with this SBRT schedule.^{12,34} It should be noted that in the present nonrandomized study SDRT was associated with smaller tumors, greater percentage of prostate cancer and lower percentage of lymph node oligometastases, which could affect the baseline PET avidity in the SBRT cohort. Nonetheless, the impact of the BED on local control of the 2 treatment regimens used here was proven in a prospective randomized trial.⁵ Within this context, the prognostic significance of early metabolic changes postradioablation appears promising, enabling LR prediction at an early time point compared with morphologic-based imaging assessments. The demonstration of LR prediction at 3 months postablation failure provides a basis for prospectively designed clinical trials testing the hypothesis that a timely ablative consolidation of detectable OM lesions mitigates metastatogenicity, improving the cure of early metastatic cancer.

References

- Hellman S, Oligometastases Weichselbaum RR. *J Clin Oncol*. 1995;13:8–10.
- Iyengar P, Wardak Z, Gerber DE, et al. Consolidative radiotherapy for limited metastatic non-small-cell lung cancer. *JAMA Oncol*. 2018;4: e173501.
- Palma DA, Olson R, Harrow S, et al. Stereotactic ablative radiotherapy versus standard of care palliative treatment in patients with oligometastatic cancers (SABR-COMET): A randomised, phase 2, open-label trial. *Lancet*. 2019;393:2051–2058.
- Gomez DR, Tang C, Zhang J, et al. Local consolidative therapy vs. maintenance therapy or observation for patients with oligometastatic non-small-cell lung cancer: Long-term results of a multi-institutional, phase II, randomized study. *J Clin Oncol*. 2019;37:1558–1565.
- Zelevsky MJ, Yamada Y, Greco C, et al. Phase 3 multi-center, prospective, randomized trial comparing single-dose 24 Gy radiation therapy to a 3-fraction SBRT regimen in the treatment of oligometastatic cancer. *Int J Radiat Oncol Biol Phys*. 2021;110:672–679.
- Foray N, Arlett CF, Malaise EP. Radiation-induced DNA double strand breaks and the radiosensitivity of human cells: A closer look. *Biochimie*. 1997;79:567–575.
- Bodo S, Campagne C, Thin TH, et al. Single-dose radiotherapy disables tumor cell homologous recombination via ischemia/reperfusion injury. *J Clin Invest*. 2019;129:786–801.
- Greco C, Fuks Z. Forging new strategies in the cure of human oligometastatic cancer. *JAMA Oncol*. 2020;6:659–660.
- Greco C, Zelevsky MJ, Lovelock M, et al. Predictors of local control after single-dose stereotactic image-guided intensity-modulated radiotherapy for extracranial metastases. *Int J Radiat Oncol Biol Phys*. 2011;79:1151–1157.
- Greco C, Kolesnick R, Fuks Z. Conformal avoidance of normal organs at risk by perfusion modulated dose sculpting in tumor single dose radiotherapy. *Int J Radiat Oncol Biol Phys*. 2021;109:288–297.
- DeLuca PM, Report Seltzer SM. 83: Prescribing, recording and reporting photon-beam intensity-modulated radiation therapy (IMRT). *JICRU*. 2008;8:1.
- Greco C, Pares O, Pimentel N, et al. Phenotype-oriented ablation of oligometastatic cancer with single dose radiation therapy. *Int J Radiat Oncol Biol Phys*. 2019;104:593–603.
- Greco C, Pares O, Pimentel N, et al. Early posttreatment PET SUV_{max} predicts local control following single dose radiation therapy (SDRT) in oligometastasis. *Int J Radiat Oncol Biol Phys*. 2015;93: E599–E600.
- Wahl RL, Jacene H, Kasamon Y, Lodge MA. From RECIST to PERCIST: Evolving considerations for PET response criteria in solid tumors. *J Nucl Med*. 2009;50(suppl 1):122–150.
- Contal C, O'Quigley J. An application of changepoint methods in studying the effect of age on survival in breast cancer. *Comput Stat Data Anal*. 1999;30:253–270.
- Youland RS, Packard AT, Blanchard MJ, et al. ^{18}F -FDG PET response and clinical outcomes after stereotactic body radiation therapy for metastatic melanoma. *Adv Radiat Oncol*. 2017;2:204–210.
- Solanki AA, Weichselbaum RR, Appelbaum D, et al. The utility of FDG-PET for assessing outcomes in oligometastatic cancer patients treated with stereotactic body radiotherapy: A cohort study. *Radiat Oncol*. 2012;7:1.
- Choi J, Kim JW, Jeon TJ, Lee IJ. The ^{18}F -FDG PET/CT response to radiotherapy for patients with spinal metastasis correlated with the clinical outcomes. *PLoS One*. 2018;13:1–12.
- Mazzola R, Fersino S, Alongi P, et al. Stereotactic body radiation therapy for liver oligometastases: Predictive factors of local response by ^{18}F -FDG-PET/CT. *Br J Radiol*. 2018;91: 20180058.
- Pitroda SP, Weichselbaum RR. Integrated molecular and clinical staging defines the spectrum of metastatic cancer. *Nat Rev Clin Oncol*. 2019;16:581–588.
- Bakhoun SF, Cantley LC. The multifaceted role of chromosomal instability in cancer and its microenvironment. *Cell*. 2018;174:1347–1360.
- Sun B, Brooks ED, Komaki R, et al. Long-term outcomes of salvage stereotactic ablative radiotherapy for isolated lung recurrence of non-small cell lung cancer: A phase II clinical trial. *J Thorac Oncol*. 2017;12:983–992.
- Meijneke TR, Petit SF, Wentzler D, Hoogeman M, Nuytens JJ. Reirradiation and stereotactic radiotherapy for tumors in the lung: Dose summation and toxicity. *Radiation Oncol*. 2013;107:423–427.
- Ogawa Y, Shibamoto Y, Hashizume C, et al. Repeat stereotactic body radiotherapy (SBRT) for local recurrence of non-small cell lung cancer and lung metastasis after first SBRT. *Radiat Oncol*. 2018;13:136.
- Caivano D, Valeriani M, De Matteis S, et al. Re-irradiation in lung disease by SBRT: A retrospective, single institutional study. *Radiat Oncol*. 2018;13:87.

26. Benedict SH, Yenice KM, Followill D, et al. Stereotactic body radiation therapy: The report of AAPM Task Group 101. *Med Phys*. 2010;37:4078–4101.
27. Withers HR, Taylor JM, Maciejewski B. Treatment volume and tissue tolerance. *Int J Radiat Oncol Biol Phys*. 1988;14:751–759.
28. Trovo M, Minatel E, Durofil E, et al. Stereotactic body radiation therapy for re-irradiation of persistent or recurrent non-small cell lung cancer. *Int J Radiat Oncol Biol Phys*. 2014;88:1114–1119.
29. Sahgal A, Ma L, Weinberg V, et al. Reirradiation human spinal cord tolerance for stereotactic body radiotherapy. *Int J Radiat Oncol Biol Phys*. 2012;82:107–116.
30. Hashmi A, Guckenberger M, Kersh R, et al. Re-irradiation stereotactic body radiotherapy for spinal metastases: A multi-institutional outcome analysis. *J Neurosurg Spine*. 2016;25:646–653.
31. Thibault I, Campbell M, Tseng CL, et al. Salvage stereotactic body radiotherapy (SBRT) following in-field failure of initial SBRT for spinal metastases. *Int J Radiat Oncol Biol Phys*. 2015;93:353–360.
32. Hoopes DJ, Tann M, Fletcher JW, et al. FDG-PET and stereotactic body radiotherapy (SBRT) for stage I non-small-cell lung cancer. *Lung Cancer*. 2007;56:229–234.
33. Henderson MA, Hoopes DJ, Fletcher JW, et al. A pilot trial of serial 18F-fluorodeoxyglucose positron emission tomography in patients with medically inoperable stage I non-small-cell lung cancer treated with hypofractionated stereotactic body radiotherapy. *Int J Radiat Oncol Biol Phys*. 2010;76:789–795.
34. Hong JC, Ayala-Peacock DN, Lee J, et al. Classification for long-term survival in oligometastatic patients treated with ablative radiotherapy: A multi-institutional pooled analysis. *PLoS One*. 2018;13: e0195149.